The Journal of the Oceanological Society of Korea
Vol. 19, No. 2, p. 141-152, December 1984

Circulation Dynamics of the Keum River Estuary*
II. Fluid Dynamic Characteristics

Jong Yul Chung and In Kweon Bhang
Dept. of Oceanography, Seoul National University, Seoul 151

錦江 河口의 海水循環力學
第2報. 流體力學的 諸特性

鄭 鍾 律·方 仁 權
서울大學校 海洋學科

Abstract: In order to investigate the circulation dynamics of the Keum River estuary, 300 velocity fields obtained at six sites over two tidal cycles by using instantaneous profiling technique were analyzed in detail.

In this investigation, the variability of shear velocity, bottom shear stress, drag coefficient, and roughness length scale were confirmed. The measured values of the bottom boundary drag coefficient show wide range of variations, i.e., $C_{100}=6.78\times10^{-5}\sim1.15\times10^{-1}$, and the mean of 300 measurements is 1.6×10^{-2}. The relationship between U_* and C_{100} also show the scatter in values. However, overall mean values over two tidal cycles at 6 stations show that if $U_*\lesssim1$cm/s, C_{100} is unpredictable, if $U_*\gtrsim1$cm/s, C_{100} increase with U_*. The values of Re_{100} and C_{100} have scatter. But the overall mean values over two tidal cycles show that if $Re_{100}\lesssim3.6\times10^5$, C_{100} is unpredictable, if $Re_{100}\gtrsim3.6\times10^5$, $C_{100}=1.4\times10^{-2}$.

Finally the flow regime of the Keum River estuary was classified as "subcritical fully turbulent" flow.

要約: 금강하구의 6개 정점에서 대·소조기때 순간물리장 측정기법으로 25시 동시관측된 300개의 유속장을 분석하여 흐름에 대한 유체역학적 제특성을 규명했다.

본 연구결과, 마찰속도, 저면마찰응력, 저면마찰계수 및 거칠기높이 등이 크기의 차수 이상의 범위로 변하며 분산됨이 밝혀졌다. 저면마찰계수는 $6.78\times10^{-5}\sim1.15\times10^{-1}$의 변화폭을 나타내고 전 관측치의 평균은 $\simeq1.6\times10^{-2}$이다. 마찰속도와 저면마찰계수 사이에도 분산이 나타나고 있다. 두 조석주기에 대해 평균을 취한값에서는 $U_*\lesssim1$cm/s이면 C_{100}은 그 값을 예측하기 어렵게 변하지만, $U_*\gtrsim1$cm/s이면 C_{100}은 U_*와 비례하여 증가됨이 밝혀졌다. 또한 $Re_{100}\lesssim3.6\times10^5$구간에서는 C_{100}은 예측불가이지만 $Re_{100}\gtrsim3.6\times10^5$구간에서는 $\simeq1.4\times10^{-2}$을 나타냈다.

본 연구에서 밝혀진 유체역학적 제특성에 근거하여 금강하구의 흐름을 규정한다면 이는 완전 난류상태의 상류임이 밝혀졌다.

INTRODUCTION

Over the past thirty years a relatively small number of studies of the estuarine circulation have been published. Bowden(1974) studied the estuarine circulation, especially on the ebb tidal circulation in the Mersey Estuary. After Bow-

Manuscript received 24 April 1984, revised 22 September 1984.
* This research was supported by the Basic Science Implementation Fund(Ministry ofEducation: 80), the Graduate Implementation Fund (Ministry of Education: 82), and the Agricultural Development Agency (RIBS-TC-82-503).

den's work, Sternberg(1968), Seitz(1973), Gordon(1974), Heathersaw(1974), and Chung (1979) tried to understand the physics of the estuarine circulation.

The remaining problems in the estuarine circulation can be summarized as follows; (1) the variability of bottom stress (2) the wide variation of the drag coefficient (3) the turbulent structure, especially in the boundary layer. These problems require accurate evaluation of boundary layer stress with flow rate, bed forms, mobility of beds, and nature of sedimentary deposits.

In summary, the priority of the estuarine study goes to the velocity profiles, determining the shear stress distributions in the vertical and its boundary value. The measurement of shear stress is important because of its relationship in revealing the fluid dynamic problems.

Although observations in the estuaries suggest that there are many physical processes at work, and some of which are better understood than others in contrast with the open oceanic observations, the flow fields in estuaries have not been extensively studied, despite its increasing importance.

This study is an attempt to determine and describe some of the turbulent process in a partially mixed estuary as the second part of series of works on the Keum River estuary (Chung, 1981, Chung, Lee and An, 1983b). The processes are identified by the study of instantaneous velocity fields.

The uniqueness of this study lies in the inclusion of the detailed analysis of flow dynamics to reveal the variability of the roughness length scale and the wide variation of the drag coefficient along with the variability of the shear velocity which has close relationship with the boundary shear stress, flow rate, bed form, and mobility of beds.

The Keum River estuary is located in the

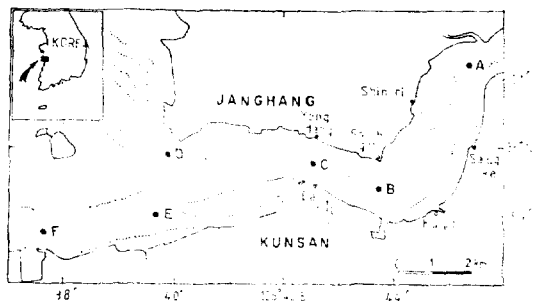

Fig. 1. Station map (dotted line denotes the low tidal boundary).

middle of the western coast of the Korean peninsula. The Keum River which empties the southeastern part of the Yellow Sea has the total drainage area of approximately 10,000 km². The average annual river runoff is about 6.4×10^9 metric tons and about 60% of total runoff flows during July, August, and September.

Figure 1 shows the location of the measurement site. Tides in the area have spring tidal range of 5.74 m and are of the semidiurnal type with diurnal inequality. At maximum strength, the maximum current reaches 200 cm/sec at the entrance of the Keum River. The ratio of M4/M2 is 0.44~1.92. In general, the ebb current are stronger than the flood current. At the entrance of the Keum River, the maximum flood current appears at 2.4~3.1 hours after the low water and the maximum ebb current appears at 3.5~4.7 hours after the high water. The ebb tide lasts about 6.4~7.5 hours.

Most natural flows that transport sediment and suspended matter are turbulent. Therefore, to reveal the nature of the circulation of the estuary, we have to design an experiment, which can deal the turbulence problems. With turbulent flow it is impossible to solve equations of motion to obtain exact solutions for such things as boundary resistance or velocity profiles in turbulent flows. Most of equations on turbulent flow are semi-empirical in nature, although the general form of the equation may be suggested either by dimensional analysis or by the

certain qualitative or "phenomenological" theories. Therefore the numerical constants in the equation and its specific form must be supplied by experimetns.

As reasoned above, in dealing the flow dynamics, only workable technique is the reliable measurement of instantaneous velocity profiles. But it is very difficult to make detailed observations of the scales, shapes, motions, and interactions of eddies, especially the relatively small eddies near boundary. Therefore, an instantaneous velocity profiling technique was adopted by designing near bottom measurement over tidal cycle along with temperature and salinity. Our scheme of observations are shown in Fig. 1 (Chung et al. 1983b).

DATA REDUCTION PROCEDURES

The simultaneous observations were carried out at 3 stations for 25 hours using the instantaneous profiling method. During the neap tide (June 15~17) Stations D, E and F were visited first and Stations A, B and C, the next day. During the spring tide (June 22~24), observations were made at Stations A, B and C and the next day at Stations D, E and F.

The instruments used measuring the instantaneous velocity field were CM-2 and DCM-2 type(Toho Dentan Co.) current meter and temperature and salinity were measured by NIO T-S and T-S bridge (Hydro-Bios Co. Model MC-5) which were hold 1 m above the current meter. And water samples were obtained every hour for calibration.

Temperature and Salinity

The temperature variations were neglected because the accuracy of NIO T-S is ± 0.001°C and the temperature fluctuations in the estuary are small and generally neglected in the estuarine circulation.

The water samples were obtained in order to calibrate the salinity measured by NIO T-S bridge. The salinity of the water samples was determined by Autosalinometer (Guildline Co. Model 8400). The errors of salinity were negligible at stations C and F. But there's 1% difference at stations A and E, so it was calibrated by the regression method. And at Stations B and D, electrical conductivity was observed, and converted to salinity by Bennett's (1976) formula using the IBM 370/125 cocomputer.

Correction of current speed and calculation of streamwise and cross-streamwise component

Two CM-2 type and one DCM-2 type current meters were used. The actual depth of the current meter during the observation was determined by the wire angle measured at every observation.

The streamwise and cross-streamwise direction were determined by the depth and time average of the current velocity over the flood and ebb flow respectively. Those data were corrected by the amount of 6° 47'W magnetic variation increase at Kunsan. As shown in Figure 1 and Table 1 the flow directions are nearly consistent with the geometry. The X-component represent the streamwise and the Y-component the cross-streamwise flow.

FLOW REGIME AND CHARACTERISTICS

Roughness length scale, shear velocity and boundary drag coefficient

The velocity profiles for flood and ebb show the general shape of the logarithmic velocity profile. Generally, it is valid at large Reynolds

Table 1. Flow direction of flood and ebb.

St.	Spring		Neap	
	Flood	Ebb	Flood	Ebb
A	39°	202°	32°	209°
B	104°	284°	104°	282°
C	112°	296°	102°	269°
D	153°	324°	145°	330°
E	88°	242°	73°	239°
F	70°	253°	72°	250°

Table 2. Maximum, mean and rms speed in cm/sec.

St.	Spring						Neap					
	Flood			Ebb			Flood			Ebb		
	Max.	Mean	Rms	Max.	Mean	Rms	Max.	Mean	Rms	Max.	Mean	Rms
A	198	114.1	121.2	136	88.7	92.5	122	64.5	67.8	108	70.7	73.4
B	146	68.1	84.5	98	47.7	53.4	105	51.9	55.9	87	40.6	44.6
C	189	113.7	121.3	159	78.8	85.1	116	60.8	68.9	126	55.0	61.8
D	150	74.9	82.6	127	80.9	87.0	103	47.7	52.4	78	45.0	49.3
E	176	73.8	87.9	163	91.2	96.4	115	42.2	50.9	99	47.5	50.2
F	187	73.2	85.4	177	100.0	107.1	128	51.1	57.5	137	51.0	53.7

number if z/h is less than about 0.15(Tennekes and Lumley, 1972) where z denotes the height from the bottom and h, the total water depth. The values fitted with this curve were measured near bottom so the use of this expression should be valid.

The near bottom currents of the flood and ebb were fitted by least-square method to the logarithmic profile and the value of shear velocity, u_*, and roughness length scale, z_0, were obtained. And then from the relation of the shear velocity and bottom shear stress, $\tau_0=\rho u_*^2$, the bottom shear stress was computed.

In this computation it was implicitly assumed that the logarithmic profile exist at all times during when measurements were made. Bowden et. al. (1959) suggested that assuming that the logarithmic piofile exists may not be an unreasonable assumption and also Sternberg(1968) has reported that the mean occurrence of the logarithmic profile is 85% based on ±10% fit to this relationship. Chung(1979, 1981) also showed validity of the logarithmic profile at large Reynolds number. In this study it was found that the ratio of the mean occurrence of the logarithmic profile is 90% based on 10% fit to this ralationship.

The computed shear velocity, roughness length scale, bottom shear stress and drag coefficient are listed in Table 3. The shear velocity, roughness length scale, bottom shear stress and drag coefficient of this measurements, also showed the difference of more than an order of magnitude, even measured at the same site on successive flood and ebb. Therefore, it requires change of the conventional meaning of these values in fluid dynamics. Recently, Heathersaw (1974), Ludwick(1974) and Chung(1979, 1981) have reported the variability of these values and also showed that there is no clear correlation between measured values of the roughness length scale and the observed grain size characteristics.

Chung(1979) and Chung and Grosch(1980b) have suggested that the variability of the shear velocity and roughness length scale, which were believed as invariant values and determined by the grain size of the bottom, should be interpreted with the variability of flow regime, bed form, mobility of beds, and inequality of the successive flood and ebb.

Frictional interactions between tidal currents and bed

The frictional interactions between tidal currents and bed can be expressed in conventional terms by means of quadratic shear stress law;

$$\tau_0=\rho C_{100}U^2_{100}$$

Where, C_{100} is the drag coefficients, U_{100} is the mean current at 100cm above the bed and ρ is the fluid density of that depth. With $\tau_0=\rho u_*^2$

$$C_{100}=(u_*/U_{100})^2$$

The value of $u_*$and mean bottom longitudinal

Table 3. Mean values of various parameters.

St.			Spring		Neap	
			Flood	Ebb	Flood	Ebb
A	ρ	(gm/cm^3)	1.010	1.009	1.004	1.003
	ν	(cm^2/sec)	9.271×10^{-3}	9.177×10^{-3}	9.259×10^{-3}	9.234×10^{-3}
	u^*	(cm/sec)	5.54	7.38	3.88	7.74
	z_0	(cm)	0.684	1.974	1.399	2.777
	τ	(dyn/cm^2)	40.20	66.28	18.78	63.01
	C_{100}	(10^{-2})	0.516	1.103	0.757	1.457
B	ρ	(gm/cm^3)	1.014	1.015	1.011	1.010
	ν	(cm^2/sec)	9.571×10^{-3}	9.609×10^{-3}	9.652×10^{-3}	9.593×10^{-3}
	u^*	(cm/sec)	9.67	5.77	5.82	3.94
	z_0	(cm)	3.000	4.346	2.836	5.229
	τ	(dyn/cm^2)	119.1	41.57	45.90	17.18
	C_{100}	(10^{-2})	1.528	2.146	1.351	2.075
C	ρ	(gm/cm^3)	1.017	1.013	1.013	1.011
	ν	(cm^2/sec)	9.688×10^{-3}	9.454×10^{-3}	9.713×10^{-3}	9.572×10^{-3}
	u_*	(cm/sec)	10.68	9.63	4.33	5.33
	z_0	(cm)	1.736	3.589	4.074	4.125
	τ	(dyn/cm^2)	192.8	111.2	24.42	39.37
	C_{100}	(10^{-2})	1.290	2.252	1.346	1.691
D	ρ	(gm/cm^3)	1.019	1.017	1.016	1.015
	ν	(cm^2/sec)	9.833×10^{-3}	9.772×10^{-3}	1.002×10^{-2}	9.975×10^{-3}
	u_*	(cm/sec)	6.30	13.60	6.71	7.48
	z_0	(cm)	2.024	5.119	6.066	5.056
	τ	(dyn/cm^2)	54.81	225.1	54.03	63.07
	C_{100}	(10^{-2})	1.044	3.761	2.617	3.145
E	ρ	(gm/cm^3)	1.018	1.017	1.016	1.015
	ν	(cm^2/sec)	9.842×10	9.702×10	9.991×10	9.904×10
	u_*	(cm/sec)	4.80	5.77	1.65	3.12
	z_0	(cm)	2.142	1.655	0.789	2.086
	τ	(dyn/cm^2)	29.39	41.87	4.579	11.61
	C_{100}	(10^{-2})	0.911	0.846	0.540	1.033
F	ρ	(gm/cm^3)	1.019	1.018	1.018	1.018
	ν	(cm^2/sec)	9.916×10^{-3}	9.785×10^{-3}	1.013×10^{-2}	1.011×10^{-2}
	u_*	(cm/sec)	6.27	8.92	3.74	2.80
	z_0	(cm)	3.040	3.338	2.714	4.229
	τ	(dyn/cm^2)	89.18	110.4	16.58	12.69
	C_{100}	(10^{-2})	1.335	1.743	1.216	1.554

velocity were used in determining the C_{100} and listed in Table 3. The bottom drag coefficient also shows the difference of more than an order of magnitude, even we have measured at the same site on successive flood and ebb.

Heathersaw(1974) has reported the scatter in his measurements of drag coefficient in the Irish Sea. Ludwick(1975) has reported that there was considerable scatter in measured individual values of C_{100} and u_*, based on 620 measurem-

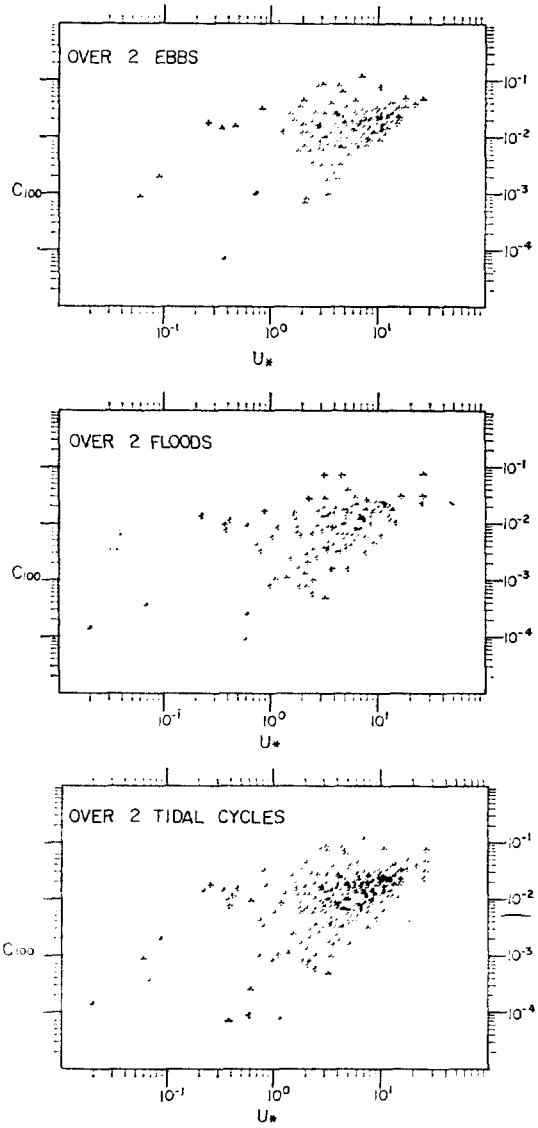

Fig. 2. C_{100} versus u_* for 300 measurements in the Keum River estuary.

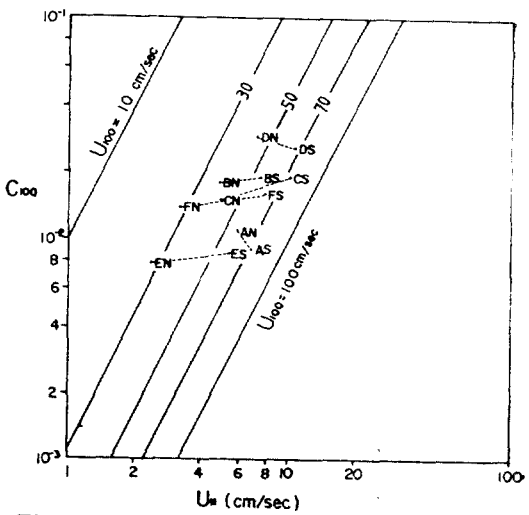

Fig. 3. Mean drag coefficient ($\bar{C}_{100}$) versus mean shear velocity ($\bar{u}_*$) over spring (S) and neap (N) tide at six stations.

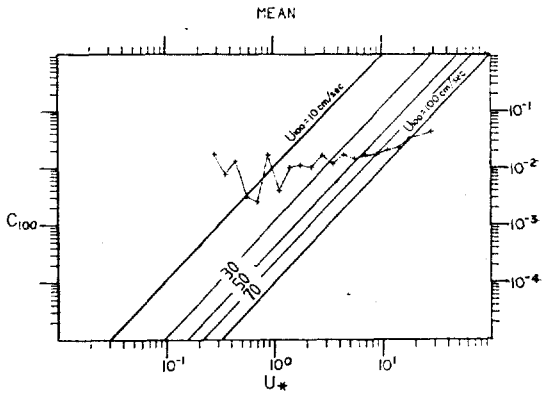

Fig. 4. Mean C_{100} versus mean u_* over 300 measurements during two tidal cycles.

ents at the entrance to Chesapeake Bay. He noted that the scatter in values suggest that, given a movable bed, a size hierarchy of mobile bed forms, a time varying flow and a lack of equilibrium between the bed and the flow, C_{100} changes continuously with the flow. This phenomenon was also reported by Chung(1979, 1981) at the Lafayette River and at the Keum River estuary.

The values of C_{100} and u_* obtained from our 300 measurements are plotted in Figure 2. The mean drag coefficient, $\bar{C}_{100}$, versus mean shear velocity, u_*, over spring and neap tide at 6 stations is shown in Figure 3. And also the $\bar{C}_{100}$ versus $\bar{u}_*$ over 300 measurements during two tidal cycles is shown in Figure 4. As we can see from Figure 2, the values are scattered, as those other worker's results. However, the Figure 4, which shows the mean state over two tidal cycles, shows that if $u_* \lesssim$ 1cm/s, the drag coefficient has large fluctuation (i.e., unpredictable) but if $u_* \gtrsim$ 1cm/s, the drag coefficient

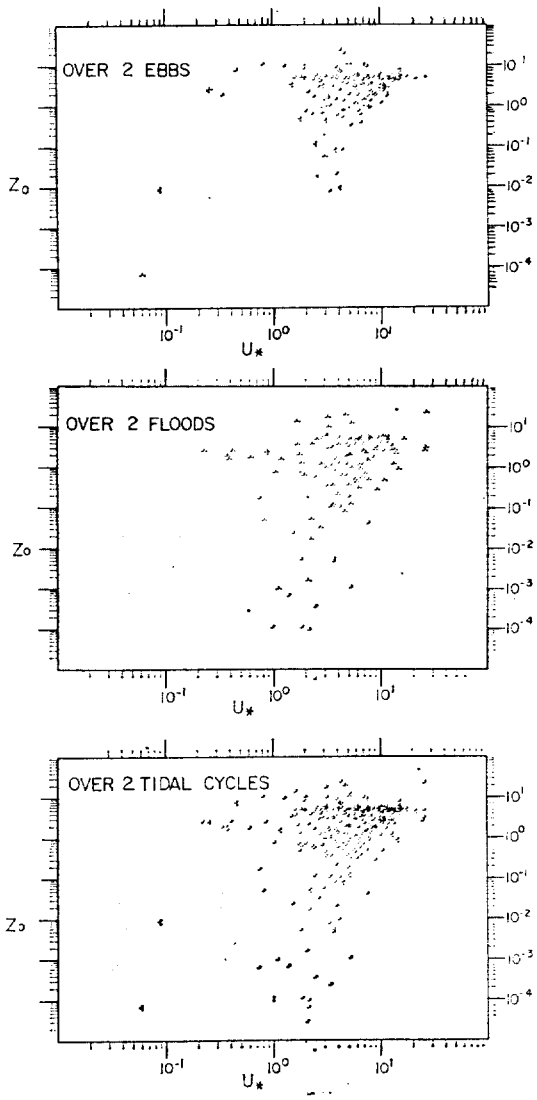

Fig. 5. z_0 versus u_* for 300 measurements in the Keum River estuary.

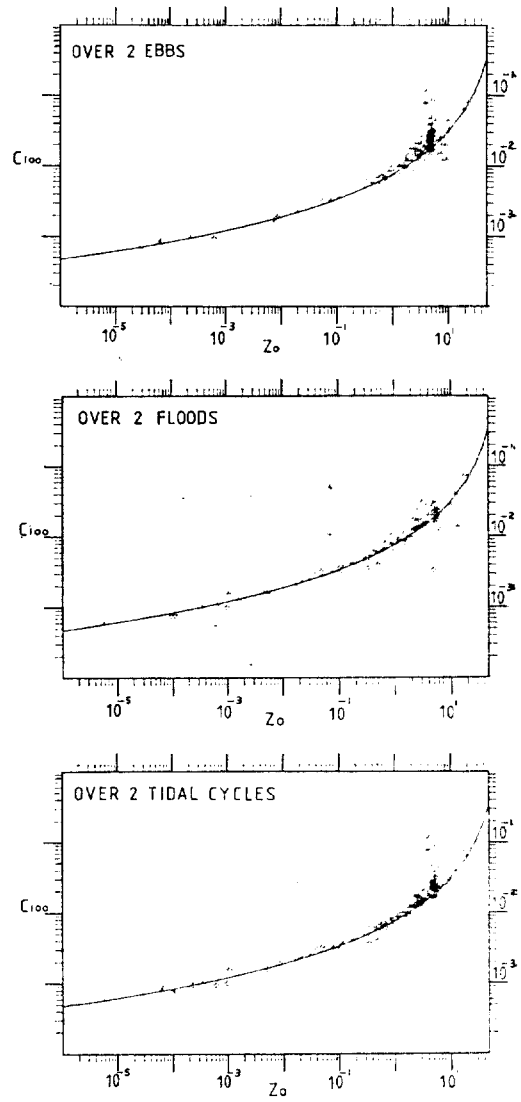

Fig. 6. C_{100} versu z_0 for 300 measurements in the Keum River estury(the line denotes $C_{100}=(k/\ln(100/z_0))^2$).

has somewhat linear relationship with u_*.

The relationship between z_0 and u_* is shown in Figure 5. The values also show considerable scatter. The C_{100} versus z_0 obtained from our 300 measurements are plotted in Figure 6 along with the value of

$$C_{100}=\left[\frac{K}{\ln(100/z_0)}\right]^2$$

to test our assumption on the existence of the logarithmic profile in the bottom boundary layer. It was found that the mean ratio of the occurence of the logarithmic profile is 90% during our measurements.

Flow charactistics

Froude number(F) : In general the regime of the flow is classified by the Froude number and Reynolds number.

$$F=\frac{U}{(gh)^{1/2}}$$

where U is the characteristic velocity, g is the gravitational acceleration and h is the depth of

the flow. If F is greater than unity the flow is called as supercritical or "shooting" flow and if F is less than unity the flow is called as subcritical or natural flow. In nature to get $F>1$ it requires a steep gradient of the bed or drastic decreasing of the flow depth. Under this condition an antinode and very large scale ripples can be formed.

Four distinct flow regimes are shown in Figure 10; sub-critical laminar, supercritical laminar, sub-critical turbulent, and supercritical turbulent flow regimes. Only the last two of practical interest, and of these, the last is the least common.

The Froude number of this experiment is listed in Table 4. Our Froude number shows an order of 0.1 and fit to unity number in estuaries. Generally the Froude number of the estuaries shows an order of 0.1 and also changes about 10%, i.e., there are no critical values of Froude number in estuaries. Therefore in estuaries it is sometimes useful to use the Densimetric Froude number in terms of the cross-sectional mean velocity associated with the river discharge.

Tabe 4. Reynolds number and Froude number.
unit: Re(10^6), F(10^{-2})

St.		Spring		Neap	
		Flood	Ebb	Flood	Ebb
A	Re	9.5	8.2	5.4	6.1
	F	12.7	12.1	7.3	9.3
B	Re	7.7	3.9	4.9	3.5
	F	10.7	6.1	5.8	4.0
C	Re	10.0	7.0	5.0	4.0
	F	14.2	10.6	6.4	6.4
D	Re	6.5	8.1	4.5	4.2
	F	9.7	13.7	7.0	6.9
E	Re	5.5	7.2	3.2	3.3
	F	8.0	10.8	4.7	5.7
F	Re	5.9	8.1	3.6	2.1
	F	7.9	11.8	5.4	5.4

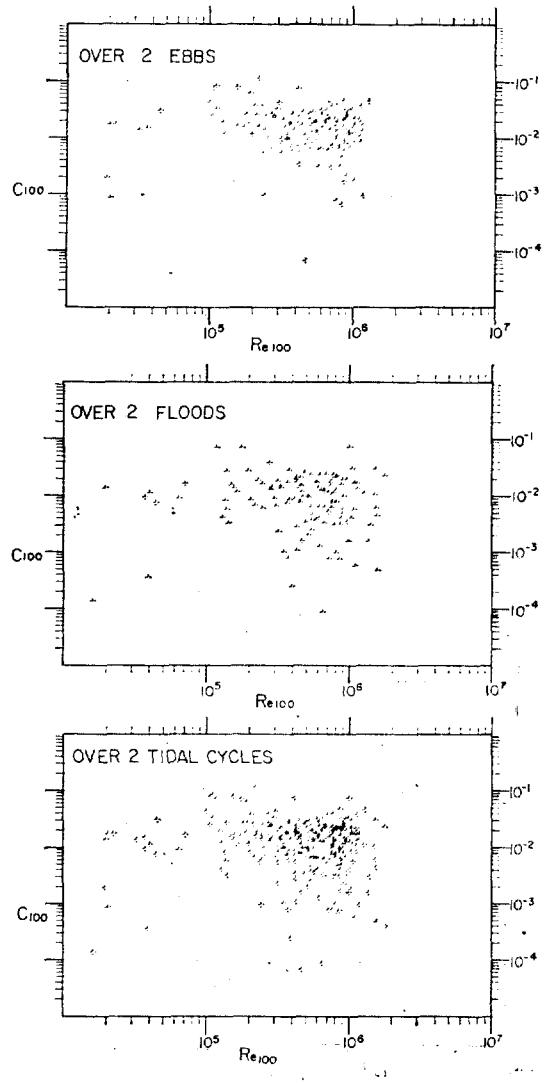

Fig. 7. C_{100} versus Re_{100} for 300 measurements in the Keum River estuary.

Reynolds number(Re) : The Reynolds number compares the relative importance of inertial and viscous forces in determining the resistance to flow.

$$Re = \frac{Uh}{\nu}$$

where ν is the kinematic viscosity, the ratio of melecular viscosity to density (μ/ρ).

The value of the Reynolds number determine whether the flow is laminar or turbulent. Below Re=2000 the flow can be laminar and above

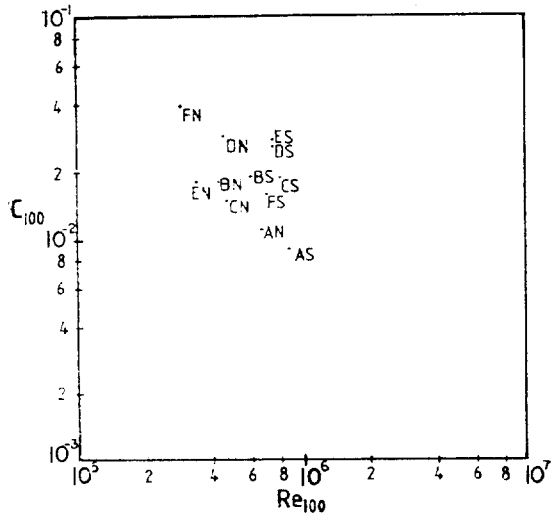

Fig. 8. Mean drag coefficient($\bar{C}_{100}$) versus mean Reynolds number($\bar{Re}_{100}$) over spring(S) and neap(N) tide at six stations.

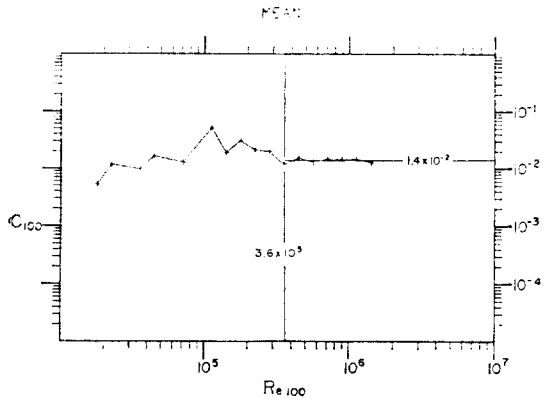

Fig. 9. Mean C_{100} versus mean Re_{100} over 300 measurements during two tidal cycles.

$Re=10^5$ the flow is likely to be fully turbulent.

Our Reynolds number shows order of 10^6. Sternberg(1968) examined the flow in a number of tidal channels and found that fully turbulent flow occurred at Re greater than 1.5×10^5 and also Chung(1978, 1981), Chung and Grosch (1980a,b, 1983a) have reported it in a well-mixed and a partially mixed estary. Our Reynolds number shows the flow is fully turbulent.

The relationship between C_{100} and Re_{100} obtained from our 300 measurements is shown in Figure 7. And the mean values of C_{100} and Re_{100} for different tidal phase is shown in Figure

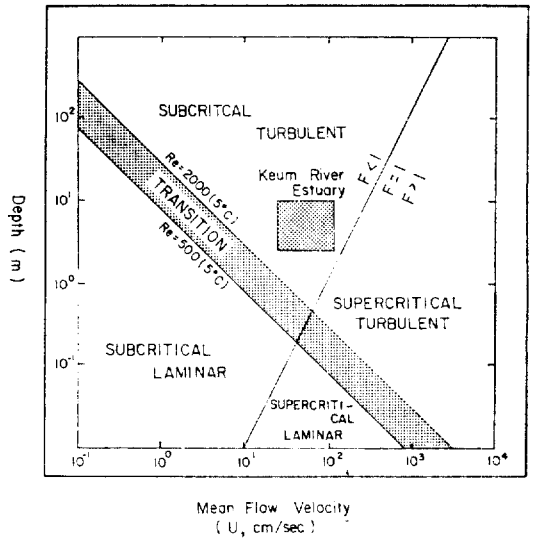

Fig. 10. Flow regime.

8. The overall mean C_{100} versus mean Re_{100}, i.e., mean values over 300 measurements during two tidal cycles, is shown in Figure 9. Figure 7 and 8 show considerable scatter and time variation. However, Figure 9 show that if Re_{100} $\leq 3.6\times10^5$, the drag coefficient is unpredictable but if Re_{100} $\geq 3.6\times10^5$, the drag coefficient has the value of 1.4×10^{-2}. The overall mean drag coefficient of our 300 measurements is 1.6×10^{-2} (Fig. 9). This value is bigger than the value of Chesapeake Bay, i.e., 1.3×10^{-2} (Ludwick, 1975) and Puget Sound, i.e., 3.1×10^{-3} (Sternberg, 1968).

As a result of this investigation it was found that if we classify the flow regime by aid of the Reynolds number and Froude number, the Keum River estuary shows a sub-critical fully turbulent flow(Figure 10).

Richardson number(Ri): The Richardson number is a comparison of the stabilizing force of the density stratification to the destabilizing influence of the velocity shear and can be expressed by

$$Ri=-\frac{g}{\rho}\frac{\partial\rho}{\partial z}\Big/\left(\frac{\partial u}{\partial z}\right)^2$$

Our Richardson number(i.e., local Richardson

number) shows positive values and also shows wide variation. The transition between laminar and turbulent flow occur at $Ri=0.25$ under uniform flow condition. However, in estuaries the transition occurs at higher Ri number because of non-uniform flow. And also the Richardson number undergoes wide fluctuation in any estuary, because of the difficulty in the precise measurements of density, velocity gradient and tidal variation. Therfore, even our effective local Richardson number, which was derived by taking the hourly measurements of $\partial\rho/\partial z$ and $\left(\frac{\partial u}{\partial z}\right)^2$ and averaging them over a tidal cycle(Bowden, 1962), shows the positive number, and it is not clear to determine the stratification.

Due to the difficulty in dealing with the local effective Richardson number we propose to define a layer Richardson number as follows;

$$Ri=(\Delta\rho/\rho)\ gh/u^2$$

where h is the depth of the upper layer flowing with a velocity u relative to the lower layer and $\Delta\rho$ is the density difference between the layers. Even this layer Richardson number has difficulty in determining the transition number, i.e., in estuary where flow is not uniform, any of Ri number is not good in determining the flow characteristics.

Friction Reynolds number(R_*) and boundary layer Reynolds number(R_{ed}): It should be noted that the result reported by Hinze(1959) was for flows over smooth boundaries at $R_*=3000$ in the laboratory experiment, while these measurements show that R_* is order of 10^5. Chung (1979), Chung and Grosch(1980a,b) have reported that the turbulent intensity may be increased as R_* increases and that the rough boundary would also increase the turbulent intensity.

The boundary layer Reynolds number of this field experiment shows very wide range of variaton depending upon the flow state. The value of the boundary layer Reynolds number indicates the degree to which the grains project into the turbulent zone of the boundary layer. Therefore, we can expect that the drag and lift on the grain will be a function of this number or ratio, particularly for values less than 5 (i.e., for hydraulically smooth boundaries).

Our results of the boundary Reynolds number indicate that, except for some of the flood case, the boundary is very rough and an intense bottom turbulence can be aroused during the ebb and slack water period. Therefore most of the sedimentological processes will occur during the ebb flow in the Keum River estuary.

Flow regime

As discussed in previous sedtions, our measured Reynolds number, friction Reynolds number, boundary layer Reynolds number and Froude number imply that the flow regime of this Keum River estuary is a fully turbulent flow. And also this fact can be verified by the Figure 10, which shows four distinct flow regimes on the basis of the Froude number, Reynolds number, mean flow depth and mean flow velocity.

Furthermore, if we classify the sub-critical turbulent flow regime on the basis of our measured characteristic mean flow velocity ($\bar{U}=$ 90cm/s), mean flow depth($h=6$m) and the Reynolds number($Re=$an order of 10^6), it can be sub-classified as "Subcritical fully turbulent flow regime".

TURBULENCE

Turbulence energy and intensity

During the spring tide, the flood flow has more turbulence energy and intensity than the ebb flow except for St. F at the entrance of the estuary. However, during the neap tide only the Stations A, C and E show bigger values. From these characteristics, we can see the flood flow of the spring tide is more turbulent than the ebb flow. But during the neap tide the situation is confined at the stations where

width is narrow.

Turbulent energy dissipation and turbulent viscosity

The maximum turbulent energy dissipation rate appears at St. D during the ebb flow of the spring. However, during the neap tide the maximum value appears at flood flow at the same station.

Our most interesting thing will be the vertical and horizontal turbulent diffusion coefficients. It was found that the vertical turbulent viscosity shows 86.6~419.5 cm^2/sec and the vertical turbulent diffusion coefficient shows 121.3~587.3 cm^2/sec. It is a reasonable value in the natural flow.

Another important aspect of the turbulent flow is the horizontal turbulent diffusion coefficients caused by the large eddies and velocity shears. Our computed values show that the horizontal turbulent diffusion coefficient due to the velocity shear is 1.0×10^4 cm^2/sec~5.5×10^4 cm^2/sec and the coefficient due to large eddies is 2.6×10^6~11.2×10^6 cm^2/sec. The order of magnitude is reasonable compared with other works in natural channel flows.

CONCLUSIONS

1. Through this investigation it was found that the values of u_*, z_0, τ_0, Re and C_{100} show scatter and change continuously with the flow. This phenomenon should be interpreted in terms of movable bed, size hierarchy of mobile bed forms, time varying flow and lack of equilibrium between the bed and the flow and also between the flood and ebb.

2. The measured value of the bottom boundary drag coefficient show wide range of variation, i.e., $C_{100}=6.78\times10^{-5}$~$1.15\times10^{-1}$.

3. The relationship between u_* and C_{100} shows the scatter in values. However, overall mean values over two tidal cycles at 6 stations have interesting relationship, i.e.,

if $u_*\leq1$ cm/sec, C_{100} is unpredictable

if $u_*\geq1$ cm/sec, C_{100} increases with u_*.

4. The values of Re_{100} and C_{100} have scatter. But the overall mean values over two tidal cycles also have certain tendency, i.e.,

if $Re_{100}\leq3.6\times10^5$, C_{100} is unpredictable

if $Re_{100}\geq3.6\times10^5$, C_{100} is 1.4×10^{-2}

5. The roughness length scale measurements give, $\bar{z}_0=3.189$ cm (z_0 : 0~23.58cm)

6. The shear velocity measurements give, $\bar{u}_*=6.362$ cm/s (u_* : 2×10^{-2}~26.45 cm/s)

7. The bottom shear stress measurements give $\bar{\tau}_0=63.22$ dynes/cm^2 ($\bar{\tau}_0$: 10^{-4}~712 dynes/cm^2)

8. The Froude number give an order of 0.1, Reynolds number is an order of 10^6, the frictional Reynolds number is an order of 10^5, and the turbulent energy and intensity are high, therefore, the flow regime is classified as "subcritical fully turbulent" flow.

9. Puget Sound (Sternberg, 1968) : $\bar{C}_{100}=3.1\times10^{-3}$, Chesapeake Bay (Ludwick, 1974) : $\bar{C}_{100}=1.3\times10^{-2}$, Lafayette River estuary (Chung, 1979) : $\bar{C}_{100}=4.5\times10^{-3}$, Keum River estuary (Present study) : $\bar{C}_{100}=1.6\times10^{-2}$

10. The friction Reynolds number of laboratory experiment for turbulent boundary layer on the smooth wall is $R_*=3000$. Our R_* is order of 10^5 and the ratio between the normalized turbulent intensity and the shear velocity lies in the range of 3.0~1.15 cpmpared to 2.0 of $R_*=3000$. This implies that the turbulent intensity may be increased as R_* increases and the rough boundary would also increase the turbulent intensity.

REFERENCES

Bowden, K.F., 1947. Some observations of waves and other fluctuations in a tidal current. Proc. Roy. Soc. A. 192:403-425.

Bowden, K.F., Fairbairn, L.A. and Hughes, P., 1959. The distribution of shearing stress in a tidal current. Geophys. J. Roy. Astro. Soc. 2:288-305.

Bowden, K.F., 1962. Measurements of turbulence

n ear the sea bed in a tidal current. J. Geophys. Res., 67. 8:3181-3186.

Chung, J.Y., 1979. Turbulence spectra in a well-mixed estuary. Ph. D. dist.(Old Dominion Univ.), pp. 233.

Chung, J.Y. and C.E. Grosch, 1980a. Intermittency of turbulent momentum transport in an intermediate layer, proceeding of Third International Symposium on Stochastic Hydraulics (Tokyo, Japan), Suppl. Vol., pp. 765-772.

Chung, J.Y. and C.E. Grosch, 1980b. Intermittency of turbulent momentum transport in an inner boundary layer, proceeding of the First Asian congress of fluid mechanics (Indian, Institute of Science, Bangalore, India), Vol. C. B37, p. 1-6.

Chung, J.Y. and C.E. Grosch, 1983a. Fluid dynamic implications of the intermittency of turbulent momentum transport in the oceanic turbulent boundary layer, Jr. of Oceanolog. Soc. of Korea, Vol. 18, No. 2, pp. 104-110.

Chung, J.Y., J.H. Lee, and H.S. An, 1983b. Circulation dynamics of the Keum River estuary: I. Variability of the salinity boundary layer, J. Oceanolog. Soc. of Korea, Vol. 18, No. 2, pp. 142-148.

Gordon, C.M., 1974. Intermittent momentum transport in a Geophysical boundary layer. Nature 248: 392-394.

Heathersaw, A.D., 1974. Measurements of turbulence in the Irish Sea benthic boundary layer. sp. Sci. Comm. Nato. 11-31.

Hinze, J.O., 1959. Turbulence. McGraw-Hill. pp. 440.

Lee, S.W., 1982. Report on hydrographic and bethymetric survey in Kunsan Harbour. The Kunsan port and horbour construction office, p. 39.

Ludwick, J.C., 1975. Variations in the boundary-drag coefficient in the tidal entrance to Chesapeake Bay, Virginia. J. Marine Geol. 19:19-28.

Seitz, R.C., 1973. Observations of intermediate and small scale turbulent water motion in a stratified estuary. Chesapeake Bay Inst. Tech. Rep. 79, Ref. 73-2.

Sternberg, R.W., 1968. Friction factors in tidal channels with differing bed roughness. J. Marine Geol. 6:243-260.

Tennekes, H. and Lumley, J.L., 1972. A first course in turbulence. MIT press, New York, pp. 300.